C-BAND ACCELERATOR STRUCTURE DEVELOPMENT AND TESTS FOR THE SWISSFEL

R. Zennaro, J. Alex, H. Blumer, M. Bopp, A. Citterio, T. Kleeb, L. Paly, J.-Y. Raguin
Paul Scherrer Institute, Villigen

Abstract

The SwissFEL requires a 5.8 GeV beam provided by a C-band linac consisting of 104 two-meter accelerating structures [1]. Each structure is of the constant-gradient type and is composed of 113 cups [2]. The cup shape is double-rounded to increase the quality factor. No tuning feature is implemented. For this reason ultra-precise turning is exploited. A strong R&D program has been launched on structure fabrication, which will be followed by a future technology transfer to a commercial company. The program includes the production and test of short structures that can be brazed in the existing PSI vacuum oven and will be completed with the production of the full two-meter prototype once the new full scale brazing oven, presently under construction, is operational. The status of the R&D program, including the production and power test results of the first two test structures, is reported here.

INTRODUCTION

The baseline of the R&D program includes the production and test of four short constant-impedance structures. The first and the second test structures are composed of eleven regular cells and two matching cells. Each cell geometry and volume are defined by two joined half cups. The dimensions of the regular cells are close to the one of the first regular cell of the two-meter structure prototype [2] whereas the regular cells of the third structure have a geometry close to the one of the last regular cell. The connection to the input waveguides and output loads is provided by removable mode launchers which are mechanically connected to the structure via two flanges and two RF chokes [3]; see Figure 1.

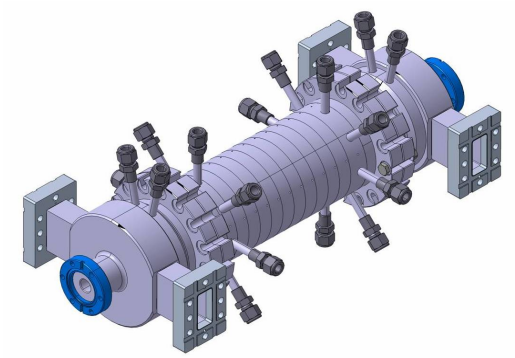

Figure 1: Short test structure.

The fourth test structure is under construction and will be equipped with an RF J-type coupler, the same type than the ones of the two-meter structure [2].

The main parameters of the test structures are summarized in Table 1.

Table 1: Main parameters of the test structures

Test Structure	Structure 1,2	Structure 3, 4
Type	Constant impedance	Constant impedance
Number of regular cells	11	11
Frequency	5.712 GHz	5.712 GHz
Phase advance/cell	2π/3	2π/3
Iris aperture radius /thickness	7.267/2.5 mm	5.478/2.5 mm
Group velocity	3.1 % c	1.4 % c
Q	10400	10350
R/Q	7214 Ohm/m	8522 Ohm/m
Nominal gradient (MV/m)	28 MV/m at 28 MW	28 MV/m at 10.84 MW

CUP PRODUCTION AND CONTROL

Extremely high accuracy in structure production is required to avoid tuning. The specified tolerance for the cup diameter is ±4 μm. In order to verify the cup size all the cups had metrology control. The histogram in Figure 2 shows the metrology results for the inner diameters of the cups produced for structure 3 and 4: the cups have a systematic error of -0.9 μm, the error distribution has a standard deviation of 0.4 μm and a peak to peak difference of 2.0 μm.

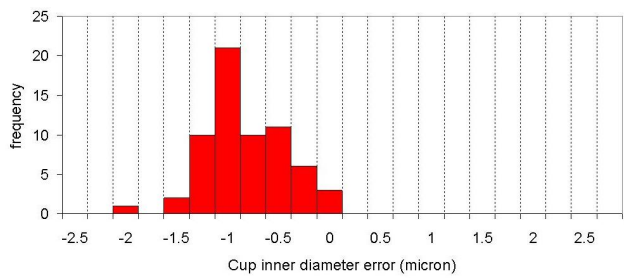

Figure 2: Histogram of the errors on the inner cup diameter for cups produced for structure 3 and 4.

To have a cheap and quick system to verify the cup dimensions we developed a single cup resonant frequency measurement tool. A resonating volume is defined by closing a half cup with a copper plate by applying a pressure of 14 MPa and by detuning the opposite half cup. The repeatability of the measurements in constant temperature conditions is excellent, with a standard deviation of the frequency of less than 5 kHz.

ISBN 978-3-95450-122-9

The cups used for structure 2 were individually controlled via metrology and RF frequency measurements. Each single cup is composed of two half cells that are individually measured.
Keeping the metrology results as reference, the frequency measurements have a systematic error of roughly 80 kHz i.e. one micron between the two halves and a random error of one micron or less.

COLD RF MEASUREMENTS

All the RF cold measurements were made in stable operating conditions obtained by cooling the structure using temperature stabilized water and by filling it with dry nitrogen.
Figure 4 shows the reflection coefficients for structure 1 (see also reference 3), 2 and 3. At the nominal frequency the reflection is respectively -31 dB for structure 1, -23 dB for structure 2 and -20 dB for structure 3.

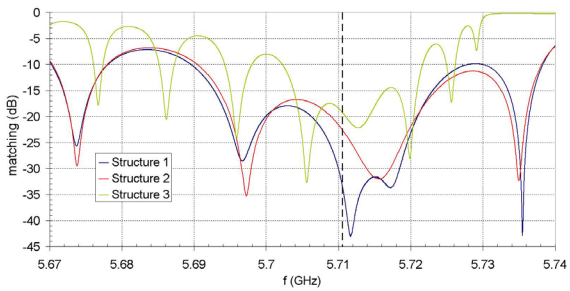

Figure 3: Reflection coefficient (S_{11}) of the three structures.

Field distributions, as shown in Figure 4, have been obtained by bead-pull measurements. Each structure was measured in two configurations, by swapping alternately the input with the output.

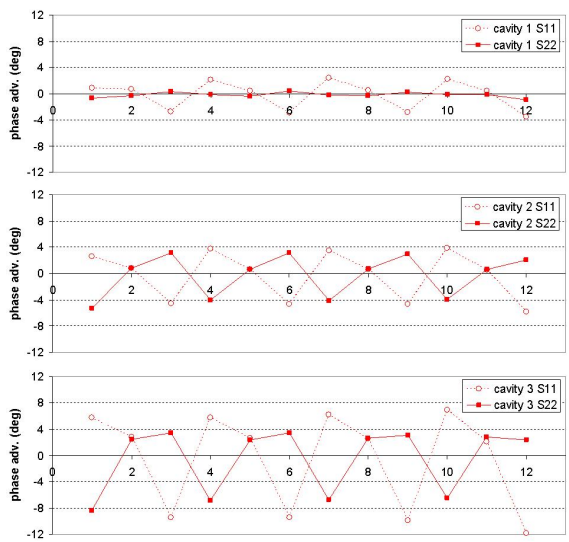

Figure 4: Error in the phase advance vs. cell number.

A standing-wave component in the field pattern is evident in the three cavity tests. This component is negligible for S_{22} in structure 1 and is very large in cavities 2 and 3 for both S_{11} and S_{22} (N.B. since the structures are fully symmetric port1 and port2 are arbitrarily defined). The three-cell periodicity in the standing-wave component is a clear indication that the mismatch is located in a single cell, either the output matching cell or the previous one.

A post-mortem inspection of structure 2 showed a brazing problem in the two matching cells; however all the regular cells were fine. Some brazing alloy penetrated into the matching cells, modifying the geometry as illustrated in Figure 5.

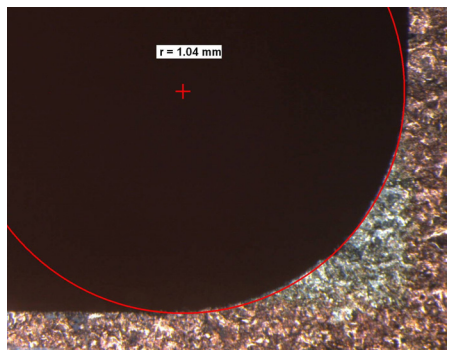

Figure 5: Fillet radius of 1 mm generated at the base of the matching iris due to brazing alloy penetration.

Unlike the regular cells where the braze joint is placed in the middle of each cell, in the matching cells, it is at the base of the matching iris. At this location, a fillet, azimuthally uniform and with a radius of roughly 1 mm, has been measured in both matching cells. As final verification the electromagnetic field distribution from the modified geometry, including the brazing error, was simulated with HFSS and the resulting error in the phase advance per cell is in good agreement with the measurements illustrated in Figure 6.

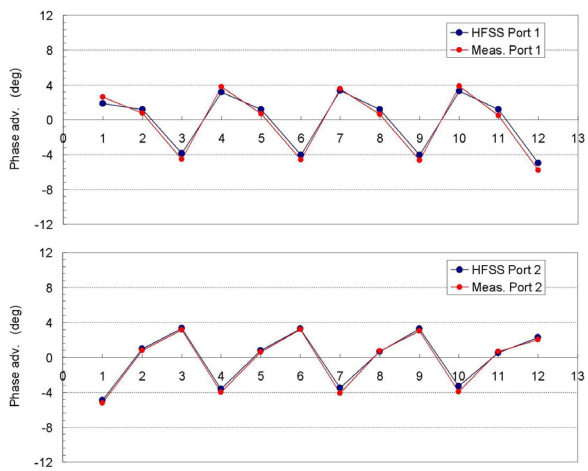

Figure 6: Error in the phase advance vs. cell number in structure 2, measure (red line) and computed (blue line) taking into account the brazing error.

ISBN 978-3-95450-122-9

CONDITIONING AND BREAKDOWN ANALYSIS

The power tests were made in TRFCB (Test RF for C-Band) which is the PSI test stand for C-band components. It is presently equipped with a SCANDINOVA K2-2S solid-state modulator and a newly developed Toshiba E37210 100-Hz 50-MW klystron which is directly connected to the structure without a pulse compressor, which is under construction.

In case of structure 1 the conditioning and power test was made at only 10 Hz. A gradient of 33.5 MV/m at the nominal pulse length (350 ns) was reached with a low breakdown rate (BDR) BDR=$8 \cdot 10^{-7}$ after 490 hours of conditioning [3]. Due to limited repetition rate it was not possible to get enough statistics to provide the dependence of the breakdown rate (BDR) on the gradient and on the pulse length.

Instead, in case of structure 2 and 3 we operated at 100 Hz; the conditioning was faster even without bake-out and after only 120 (334) hours of operation of structure 2 (structure 3) we could already acquire data for the BDR analysis.

Even operating at 100 Hz breakdowns were very rare at the nominal gradient in both structures, for this reason the pulse length dependence was studied operating almost at full klystron power; see Figure 7.

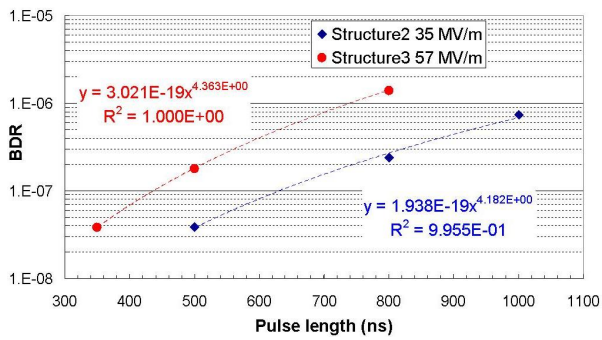

Figure 7: Pulse length dependence of BDR for structure 2 at 35 MV/m and structure 3 at 57 MV/m.

Due to the rarity of events in structures 2 and 3 and in order to have significant statistics, the BDR dependence on the gradient was measured for a pulse length of 1 μs, much longer then the nominal one (350 ns); see Figure 8.

The x-rays produced during the RF pulse were measured by a scintillator placed transversally to the structure. The integrated signal generated by the scintillator (I_s) has been acquired for different gradients. The surface field enhancement factor (β) was estimated by extrapolation from the Fowler Nordheim formula [4] by assuming I_s proportional to the emitted electrons.

A β of 68 was measured for both structures 1 and 2, by contrast structure 3 has a β of only 48.

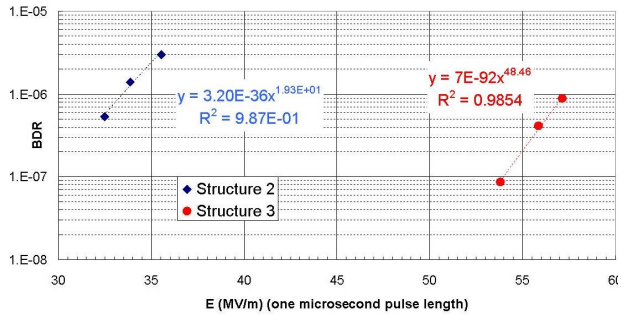

Figure 8: Gradient dependence of BDR for structure 2 and 3 for 1 μs pulse.

CONCLUSIONS AND OUTLOOK

Three of the four short test structures have been produced and power tested. The fourth structure is presently under construction; it will provide information concerning the robustness of the J-coupler design.

The machining precision required to avoid tuning has been reached and the cups are well inside the tolerances. The stacking and brazing techniques are proven for the regular cups. Some brazing problems have been encountered in the matching cells which however are not part of the nominal two-meter structure. The presence of brazing alloy in the matching cells seems to be the reason for the large phase advance error in structure 2 and for the poor matching; this problem is still under investigation. An equivalent post mortem analysis is planned for structure 3.

High accelerating gradients have been reached without difficulties and the breakdown rate is largely lower than required for operation. Breakdown localization by means of acoustic sensors is under test and will be fully operational with the two-meter prototype structure.

REFERENCES

[1] R. Ganter et al., SwissFEL CDR, PSI Bericht Nr. 10-04, April 2012.

[2] J.-Y. Raguin and M. Bopp, "The Swiss FEL C-band Accelerating Structure: RF Design and Thermal Analysis", this conference, TUPB012.

[3] R. Zennaro et al., "Design, production and power conditioning of the first C-band test accelerating structure for the SwissFEL", IPAC 2012, New Orleans, USA.

[4] R.H. Fowler and L. Nordheim, Proc. R. Soc. (London) A119, 173 (1928).